THE JOURNAL OF PHYSICAL CHEMISTRY B

ARTICLE

pubs.acs.org/JPCB

Simple One-Center Model for Linear Molecules: Application to Carbon Dioxide

Rasmus A. X. Persson*

Department of Chemistry, University of Gothenburg, SE-41296 Gothenburg, Sweden

ABSTRACT: With computational efficacy in mind, a one-center model for linear molecules is heuristically sketched. When parametrized for CO_2, all parameters save for two are supplied from literature quantum chemistry calculation or, in one case, heuristic argument. Using the remaining two adjustable parameters, the mean unsigned relative errors (predicted/observed) over the temperature range 220−290 K are 4.7% for the energy of vaporization, 0.6% for the liquid, and 8.0% for the vapor coexistence densities, respectively. The critical temperature is estimated at T_c = 308 K, the critical density at ρ_c = 0.460 g/cm^3, and the critical pressure at $p_c = 8.26 \pm 0.11$ MPa. This order of accuracy is comparable to that of many all-atom potential descriptions of CO_2 but is obtained at roughly nine times the speed. When supplied with the experimental bond length, somewhat worse agreement with experiment is exhibited for the neutron-weighted atomic pair distribution function of the liquid. This disparity is tentatively attributed to an overestimated electrostatic quadrupole−quadrupole interaction relative to the other forces present.

$$u = 4\epsilon[(\sigma\phi/r)^{12} - (\sigma\phi/r)^{6}]$$

$$2\phi = 2 + (\sigma_{\parallel}/\sigma_{\perp} - 1)(|\cos\theta_A| + |\cos\theta_B|)$$

1. INTRODUCTION

Because of their high symmetry, linear molecules are, next to the noble gas atom, the simplest target for empirical interaction potentials. A lot of simplicity is, however, sacrificed when multicenter interaction potentials are used. At the very least, the computational effort is increased quadratically with the number of interaction sites per molecule. While it may very well be argued that this at the same time increases accuracy, it is rarely investigated to what extent that is the case. In particular, it is not certain that the angular function of the dispersion interaction is correctly represented, hence introducing "false" anisotropy. Building on the work of Kihara,[1] Koide and Kihara[2] early on developed a one-center alternative to the Lennard-Jones potential for use with convex rigid bodies. Still, their model is not computationally very efficient, the primary reason being that the underlying Kihara model takes the distance between two bodies to be given by the *minimum* rather than the simpler *center-to-center* distance. The latter is quickly computed, whereas the former requires the solution of an optimization problem at each step of the molecular simulation. However, their work was a necessary first step, as the one-center Lennard-Jones potential,[3] originally conceived for the noble gas atom, when applied to molecular fluids, exhibits limited ability to capture, for instance, the vapor−liquid coexistence envelope.

As for the repulsive part of the molecular interaction, a physically very appealing model was introduced by Berne and Pechukas[4] in which the repulsive energy is proportional to the overlap volume of two spheroid bodies. Also, the dispersion attraction is anisotropic. However, owing in part to the exponential dependence that follows in that analysis, compared to simple power laws for the repulsion which need not, when properly coded, take more than a few floating point operations for each pair interaction, the model is computationally more demanding, albeit less so than the Koide−Kihara model.[2]

An interesting take on the anisotropy of molecular interactions was given by Toxvaerd,[5] building on the work of Lustig and Steele.[6] (These two latter authors were, nevertheless, not concerned with any anisotropic interaction.) In his model, specifically designed for *n*-alkanes, the basic unit of interaction is the methylene and methyl groups. The anisotropy of their interaction arises because a new interaction site, the geometric midpoint over the three nearest carbon groups, is used to calculate the energy and force on account of the original site. The *n*-alkanes studied by Toxvaerd were flexible so that the location of this point varied during the molecular dynamics simulation. This model has been subsequently parametrized to yield very good results.[7] However, it is important to realize that Toxvaerd's method does not yield any interaction anisotropy for molecular representations of high symmetry, i.e., for any molecular representation where the geometric midpoint coincides with a symmetry element. Most importantly, this includes, but is not limited to, the $D_{\infty h}$ symmetry of all homonuclear diatomics and, if treated as rigid, many linear molecules.

In this work, we introduce a simple one-center model for linear molecules that, like the Koide−Kihara[2] and Berne−Pechukas[4] models, is suited for convex rigid bodies. The efficacy of this model is illustrated when applied to CO_2. This molecule is chosen because in the study by MacRury et al.[8] it proved to be the most problematic linear molecule to fit empirically for both of the two anisotropic one-center interaction potentials they investigated. While several multicenter parametrizations have been published[9−13] of many times very great quality, the aim of this work is rather to improve upon the computational economy using a simpler model. Condensing the triatomic into one interaction site reduces in theory the number of loop iterations 9-fold and hence leads to a quite substantial speed increase, if the performance bottleneck is in the energy (or force) routines. The increased economy in both memory and computing time compared to traditional molecular models of CO_2 is the most valuable contribution of the current work. It is easy to see how

Received: May 30, 2011
Revised: July 4, 2011
Published: July 27, 2011

the development to be outlined can be applied also to oblate spheroids, but we shall concern ourselves only with the prolate case for the moment.

It is worth commenting before proceeding that some of these goals have already been achieved by a simple monocenter model for quadrupolar molecules developed by Mognetti et al.[14] For their model, experimental agreement is very good; the number of fitting parameters is small; and the model is computationally very efficient: indeed more efficient than the model to be presented here. Nevertheless, the apology for this work is that, contrary to the model to be developed here, their model is isotropic and thus contains no information at all of the orientational structure of the liquid. It is interesting to see to what extent this goal can be achieved using a coarse-grained, one-center model.

2. MOLECULAR MODEL

We start our development of the model from the regular Lennard-Jones (Mie [12-6]) potential for rare gas atoms separated by the distance r, which we write as

$$u_{LJ}(r) = 4\varepsilon\left[\left(\frac{\sigma}{r}\right)^{12} - \left(\frac{\sigma}{r}\right)^{6}\right] \tag{1}$$

where σ defines the equipotential radius and ε the maximum binding energy of the dimer. We then redefine the angular dependence of the Lennard-Jones potential such that the equipotential surface described is that of a prolate spheroid rather than a sphere. To this end, we make the substition $\sigma \rightarrow \sigma\phi(\theta_A,\theta_B)$ where

$$\phi(\theta_A,\theta_B) = 1 + \left(\frac{\sigma_\parallel}{\sigma_\perp} - 1\right)\frac{(|\cos\theta_A| + |\cos\theta_B|)}{2} \tag{2}$$

Here θ_i is the angle of the figure axis of molecule i with respect to the intermolecular axis, $\sigma_\parallel$ the length of the prolate spheroid, and $\sigma_\perp$ its width.

Next we investigate the anisotropy of the dispersion interaction in more detail. Since, per the standard London formula,[15] the strength of this interaction depends on the polarizability, and the polarizability of linear molecules is anisotropic, it follows that the binding energy should vary according to mutual orientation. Koide and Kihara[2] have dealt with the anisotropy of the interaction up to and including octupolar contributions, but the resulting expression is cumbersome and difficult to optimize for simulations as it requires many nonreducible, expensive trigonometric function evaluations. Therefore, we shall strike a compromise between accuracy and speed and derive a more general, yet simple, equation where, for a given body, we have polarizabilities specified for three orthogonal directions x, y, and z. We assume that the crossterms of the polarizability tensor vanish.

The following derivation is a slight modification of that which can be found in many textbooks.[16] Let the z-axis coincide with the intermolecular axis of two molecules, A and B. Let x and y define directions perpendicular to z and to each other. The dipole−dipole operator in this coordinate system is then

$$\hat{\mu} = \frac{1}{4\pi\varepsilon_0 r^3}(\hat{\mu}_{Ax}\hat{\mu}_{Bx} + \hat{\mu}_{Ay}\hat{\mu}_{By} - 2\hat{\mu}_{Az}\hat{\mu}_{Bz}) \tag{3}$$

where μ_{Cq} is the Cartesian q-component of the dipole operator for the dipole on molecule C and ε_0 the permittivity of free space. Assuming the molecules to have no permanent dipole moments, the first nonvanishing contribution to the energy is from the second-order perturbation correction

$$E_{att} = \sum_{n_A + n_B \neq 0} \frac{|\langle 0_A 0_B|\hat{\mu}|n_A n_B\rangle|^2}{E_{0_A 0_B} - E_{n_A n_B}} \tag{4}$$

Here $E_{n_A n_B}$ are the quantum eigenenergies of the system, described by the (arbitrary) quantum numbers n_A and n_B.

Assuming r is great, the wave functions for A and B can be taken to be approximately orthogonal, and then the matrix elements combined over both molecules can be written as products over the individual molecules. For these individual elements, strict orthogonality holds between the crossterms of the Cartesian components. Expanding the square in eq 4, we thus have

$$|\langle 0_A 0_B|\hat{\mu}_{Ax}\hat{\mu}_{Bx}|n_A n_B\rangle|^2 + |\langle 0_A 0_B|\hat{\mu}_{Ay}\hat{\mu}_{By}|n_A n_B\rangle|^2 + 4|\langle 0_A 0_B|\hat{\mu}_{Az}\hat{\mu}_{Bz}|n_A n_B\rangle|^2$$

for the numerator. Invoking the closure approximation, and replacing the square of the transition dipole expectation values with the corresponding polarizabilities, we then have

$$E_{att} \propto -\frac{1}{r^6}(\alpha^A_{xx}\alpha^B_{xx} + \alpha^A_{yy}\alpha^B_{yy} + 4\alpha^A_{zz}\alpha^B_{zz}) \tag{5}$$

To continue, a prescription for the angular dependence of the polarizability is needed. Also, it is convenient to switch to a body-fixed reference frame. To suit both these ends, we define an angle-dependent polarizability as

$$\alpha(\theta) = \alpha_\perp + (\alpha_\parallel - \alpha_\perp)|\cos\theta| \tag{6}$$

where θ is the angle between the molecular figure axis and the intermolecular axis (its cosine is quickly computed as a dot product), $\alpha_\perp$ the polarizability perpendicular to the figure axis, and $\alpha_\parallel$ that parallel to the same. In this transformation, we have restricted ourselves to the case of a linear molecule; in the general case, the polarizability would depend on two angles. Moreover, the interpolation formula that is eq 6 is a purely heuristic device. The bracketed factor in eq 5 in conjunction with eq 6 constitutes, after normalization, what we take to be the angle dependence of the ε parameter in the Lennard-Jones potential. That is, we make the replacement $\varepsilon \rightarrow \varepsilon\xi(\theta_A,\theta_B)$ in eq 1, where

$$\xi(\theta_A,\theta_B) \propto (\alpha^A_{xx}\alpha^B_{xx} + \alpha^A_{yy}\alpha^B_{yy} + 4\alpha^A_{zz}\alpha^B_{zz}) \tag{7}$$

and the $\{\alpha^A_{ii}\alpha^B_{ii}\}$ terms are given from the corresponding orientation in the body-fixed frame using eq 6. The constant of proportionality in this relation is the normalization factor which makes $\langle\xi(\theta_A,\theta_B)\rangle = 1$ when the average is taken over all possible mutual orientations. This normalization factor was computed numerically.

For linear molecules, which in general carry electric dipole moments, it is natural to include a point dipole in the interaction description, but in the case of CO_2, the first nonvanishing, asymptotic electrostatic contribution comes from the quadrupole moment. We hence approximate the electrostatic potential distribution by a linear quadrupole moment aligned along the molecular axis. The energy of interaction of two such quadrupoles is given by

$$u_{quad}(r,\theta_A,\theta_B,\psi) = \frac{3Q^2}{16\pi\varepsilon_0 r^5}(1 - 5\cos^2\theta_A - 5\cos^2\theta_B + 35\cos^2\theta_A\cos^2\theta_B + 2\cos^2\psi - 20\cos\theta_A\cos\theta_B\cos\psi) \tag{8}$$

dx.doi.org/10.1021/jp2050492 |J. Phys. Chem. B 2011, 115, 10073–10078

where Q is the quadrupole moment and ψ the angle between the two figure axes.

The resulting model is dubbed the One-Center Anisotropic plus Quadrupole (1CALJQ) potential. In the next section, we shall develop it for CO_2, but as a short digression, we must bring attention to the mixing of the 1CALJQ potential with other force fields. It is clear that mixing the 1CALJQ, as is needed in the study of mixtures, either with another potential of the 1CALJQ family or with the more common force fields that are atomically resolved over Lennard-Jones and Coulombic sites, requires new mixing rules. As this endeavour— just like in the case of atom-to-atom interaction potentials—is a subject worthy of its own study, we shall not delve too deeply into the matter. However, it is apparent after some thought that the normal Lorentz−Berthelot type mixing rules are applicable after a slight generalization. For instance, concerning ourselves with the intermixing of the 1CALJQ-type potentials—denoted A and B, respectively—it is natural to write the generalization of the Berthelot mixing rule as

$$\sigma_{\perp}^{AB} = \frac{1}{2}(\sigma_{\perp}^{A} + \sigma_{\perp}^{B}) \tag{9}$$

including the analogous equation for $\sigma_{\parallel}$. The Lorentz rule is unmodified but extended with eq 7, for which mixing is already incorporated. Indeed, already for a one-component system, the 1CALJQ fluid can be considered a (continuously changing) "mixture" of molecules of different orientation for which eq 7 provides the "mixing rule". On this generalization (or any suitable variant thereof), interfacing the 1CALJQ model with force fields of the regular all-atom Lennard-Jones variants is immediately achieved by treating each atomic Lennard-Jones interaction as a special case of the 1CALJQ interaction for which $\sigma_{\parallel} = \sigma_{\perp}$ and $\alpha_{xx} = \alpha_{yy} = \alpha_{zz} = \text{const}$.

3. TWO-PARAMETER FIT FOR CO_2

As far as possible, all parameters entering into the CO_2 model were taken from accurate theoretical predictions. Thus, the quadrupole moment was set equal to $Q = -0.89$ e Å^2, to match the accurate quantum-chemical CCSD(T) value of Maroulis,[17] and the ratio $\alpha_{\parallel}/\alpha_{\perp} = 2.07949$, to match the accurate CCSD(T) value of Haskopoulos and Maroulis.[18] Furthermore, as for the steric size of the molecule, dimensional analysis suggests that it is proportional to the polarizability. Therefore, it seems reasonable to assume that $\sigma_{\parallel}/\sigma_{\perp} = (\alpha_{\parallel}/\alpha_{\perp})^{1/3}$. This assumption is certainly not strong, but in this paper, we shall pursue it in the interest to see how far it can take us. Hence, only two parameters, no more than in the regular Lennard-Jones potential, were freely adjusted during parametrization: ε and $\sigma_{\perp}$. These were adjusted by human trial-and-error to obtain good fits for the vapor−liquid envelope over the temperature range 220−290 K. All of these simulations used 712 molecules in the Gibbs ensemble algorithm;[19] details are to be found in the Appendix. All the interaction parameters are presented in Table 1.

Table 1. Interaction Parameters for the 1CALJQ CO_2 Model

$\alpha_{\parallel}/\alpha_{\perp}$	$\sigma_{\parallel}$/Å	$\sigma_{\perp}$/Å	Q/(e Å^2)	ε/k_B/K
2.07949	4.1738166	3.27	−0.89	129

3.1. Vapor−Liquid Coexistence. The vapor−liquid equilibrium properties were used for parametrization purposes and, while not perfect, are seen to be in good agreement with observation in Table 2. A graphical display of the coexistence densities is shown in Figure 1. The mean unsigned relative error in the temperature range 220−290 K is 4.7% for the evaporation energy, $\Delta_{vap}U$, 0.6% for the liquid densities, ρ_l, 8.0% for the vapor densities, ρ_v, and 7.7% for the vapor pressure p_v. These relative errors are greater than, yet still comparable to, those reported by Merker et al.[13] for their three-center Lennard-Jones plus quadrupole (3CLJQ) CO_2 model. However, it must be kept in mind that these results have been obtained for a less computationally demanding model, parametrized using only two adjustable parameters. (Merker et al.[13] allowed six parameters to vary during their automated optimization.) It is obvious that the experimental agreement can be further improved for the 1CALJQ model if either $\sigma_{\parallel}$ or Q is turned into an adjustable parameter.

The critical temperature is slightly overestimated by the resulting model. Using the data points at 290 and 295 K, it is

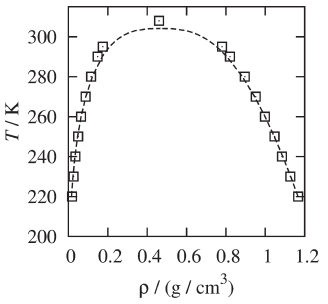

Figure 1. Phase diagram over the vapor−liquid coexistence densities. The dashed line corresponds to the empirical equation of state of ref 20. The squares correspond to the 1CALJQ CO_2 results.

Table 2. Liquid ρ_l and Vapor Density ρ_v in g/cm^3, Energy of Evaporation $\Delta_{vap}U$ in kJ/mol, and Vapor Pressure p_v in MPa at the Vapor−Liquid Coexistence at Temperature T/K for the 1CALJQ CO_2 Model and Reference Values[21a]

T	$\rho_{l,calcd}$	$\rho_{l,exptl}$	$\rho_{v,calcd}$	$\rho_{v,exptl}$	$\Delta_{vap}U_{calcd}$	$\Delta_{vap}U_{exptl}$	$p_{v,calcd}$	$p_{v,exptl}$
220	1.166(2)	1.166	0.0185(2)	0.01582	12.68(2)	13.53	0.704(4)	0.5991
230	1.127(2)	1.129	0.0264(2)	0.02327	11.98(2)	12.78	1.023(6)	0.8929
240	1.084(2)	1.089	0.0355(2)	0.03330	11.25(2)	11.98	1.395(8)	1.283
250	1.047(2)	1.046	0.0499(4)	0.04664	10.52(2)	11.12	1.95(2)	1.785
260	0.998(2)	0.9989	0.0643(4)	0.06442	9.72(2)	10.18	2.51(2)	2.419
270	0.951(2)	0.9458	0.0877(6)	0.08837	8.81(2)	9.122	3.35(2)	3.203
280	0.897(2)	0.8836	0.1157(9)	0.1217	7.84(2)	7.885	4.27(3)	4.161
290	0.821(3)	0.8047	0.149(2)	0.1720	6.63(3)	6.329	5.28(4)	5.318
295	0.781(3)	0.7526	0.175(2)	0.2097	5.91(3)	5.312	5.94(4)	5.982

[a] For the calculated values, the bracketed number indicates the uncertainty in the last digit.

dx.doi.org/10.1021/jp2050492 |J. Phys. Chem. B 2011, 115, 10073–10078

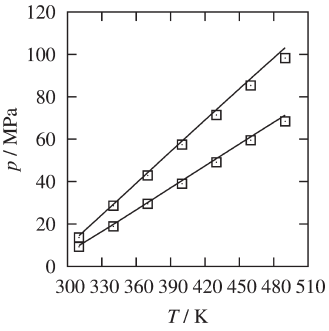

Figure 2. 1CALJQ CO_2 (squares) and experimental CO_2 (ref 20, line) supercritical pressures as a function of temperature. The upper set of data corresponds to a density of 0.7952 g/cm^3; the lower set of data corresponds to a density of 0.6764 g/cm^3. Both densities are well above the critical one. The statistical uncertainty in the calculated values is smaller than the size of the squares used to denote the points.

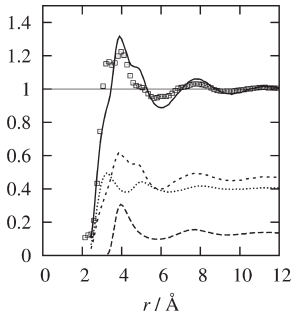

Figure 3. Neutron scattering CO_2 pair distribution function at 240 K and 1.090 g/cm^3. Solid line is $G(r)$ according to 1CALJQ CO_2; squares are experimental results from ref 24. For the 1CALJQ model are also shown: $g_{CC}(r)$ (long dashes), $g_{CO}(r)$ (short dashes), and $g_{OO}(r)$ (dots).

extrapolated to 308 K, assuming a critical exponent of $\beta = 0.32$. This constitutes a relative error of about 1%, compared to the experimental value[20] of 304.1282 K. Using all of the data points, the law of rectilinear diameters then estimates the critical density as $\rho_c = 0.460$ g/cm^3, which should be compared with the experimental value[20] of 0.4676 g/cm^3 and is slightly more erroneous. Finally, the critical pressure is estimated from a canonical Monte Carlo simulation at the critical temperature and density to be 8.27 ± 0.11 MPa; the experimental value[20] is 7.3773 MPa. The estimated critical point is shown in Figure 1 with the rest of the coexistence points.

3.2. Homogenous Region. We now briefly turn our attention to the supercritical states of CO_2. In Figure 2 we show the calculated pressure at a number of different supercritical state points, covering densities of 0.7952 and 0.6764 g/cm^3—both well above the critical density—and illustrate how it compares with the experimental data of Span and Wagner.[20] It is clear that the experimental agreement is very good with the average relative error being 4.6% for the data points sampled. This order of accuracy is comparable to that obtained for the vapor−liquid envelope and indicates that the two-parameter one-center parametrization holds validity beyond its immediate parametrization target.

3.3. Liquid Structure. Assuming a fixed bond length of the experimental value[22,23] 1.16 Å, the atomic pair distribution functions $g_{CC}(r)$, $g_{CO}(r)$, and $g_{OO}(r)$, representing the carbon−carbon, carbon−oxygen, and oxygen−oxygen distribution functions, can

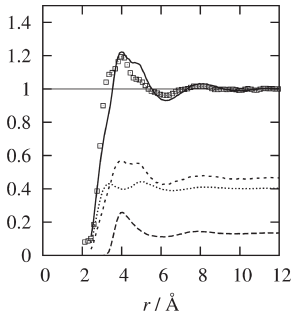

Figure 4. Same as Figure 3 but for 312 K and 0.830 g/cm^3.

Table 3. Second Virial Coefficients for the 1CALJQ CO_2 Model and Experimental Values in Units of cm^3/mol

T/K	1CALJQ CO_2	Dushek et al.[28]
220.00	−202.6(7)	−247.50
240.00	−168.4(6)	−202.83
260.00	−144.5(6)	−168.92
280.00	−122.4(5)	−142.70
300.00	−107.2(5)	−121.70
340.00	−80.6(5)	−90.57
423.15	−48.8(4)	−51.25
448.15	−42.0(4)	−43.51

be derived from "atomic sites" projected onto the model. From these, the neutron-weighted pair correlation function $G(r)$ was calculated from

$$G(r) = 0.403g_{OO}(r) + 0.464g_{CO}(r) + 0.133g_{CC}(r) \quad (10)$$

and compared with experimental results of Cipriani et al.[24] The result of this endeavor is shown in Figure 3 for a subcritical and in Figure 4 for a supercritical thermodynamic state. These simulations were run at constant volume to increase the statistical resolution of the pair distribution curve.

At 240 K, the agreement is fair but not good. The experimental data show a peak shoulder, most likely corresponding to the shortest intermolecular O−O scattering vector, at around 3 Å, right before the main peak at around 4 Å. This feature is weaker in the 1CALJQ model, to the extent of being barely visible. This suggests that the relative strength of the electric quadrupole moment is overestimated relative to the other interactions present. In particular, the linear conformation, anisotropically favored by $\xi(\theta_A,\theta_B)$, is not low enough in energy. Quantum mechanical calculation on the CO_2 dimer confirms that there should be an attractive energy for this conformation.[25]

The situation is basically the same at 312 K and 0.830 g/cm^3, but the 1CALJQ model fares better because the structure in both the experimental fluid and in the 1CALJQ fluid is partly eradicated. The quadrupole−quadrupole interaction is no longer as dominating relative to the other interactions. Still, agreement is far from perfect, as is most evident in that the shoulder on the right-hand side of the first peak in the experimental data is, while present in the 1CALJQ data, severely overestimated. Part of the reason for this overstructuring of the liquid evidenced by the 1CALJQ model can be attributed to its overestimated binding energy near the critical temperature which, as a consequence, is itself overestimated.

3.4. Second Virial Coefficients. An interesting property of any molecular model is its virial coefficients, as these give a direct indication of the quality of the few-body interaction. In a recent survey[26] of five different pair potentials of CO_2, it was found for all these models that the virial coefficients were underestimated in their magnitude, despite that at least some of these models exhibit very good vapor−liquid equilibrium envelopes. As the 1CALJQ CO_2 is also a pair potential, taking no account of many-body effects, we expect a similar result here. Indeed, this is found to be the case, as illustrated in Table 3, where the second virial coefficients, $B(T)$, have been calculated to within near negligible uncertainty by the Mayer sampling algorithm.[27] The virial coefficients calculated differ only marginally from those reported for many all-atom CO_2 models[26] and are once again an indication that good vapor−liquid equilibrium properties are not a guarantor for good virial coefficients.

These calculations also provide a useful benchmark for the speed of computating the intermolecular interaction energy. While it is clear that for large systems the monocenter potential will always be more efficient, calculating the trigonometric operations involved in the anisotropic part of its interaction adds some overhead. Consequently, the speed of execution of the two-body system, far from being nine times as efficient, is only but 1.4 times the speed of a regular CO_2 model composed of Lennard-Jones sites and atomic point charges.

4. CONCLUDING DISCUSSION

It has been demonstrated that a one-center model of the CO_2 molecule is viable for the description of the fluid of this linear molecule. Using a two-parameter fit, for the vapor−liquid equilibrium in the temperature range 220−290 K, the mean unsigned deviation (predicted/reference) errors are 0.6% for the liquid density, 4.7% for the energy of vaporization, 8.0% for the vapor density, and 7.7% for the vapor pressure. It seems beyond doubt that even better agreement, with a greater set of properties, is possible to achieve if in addition to $\sigma_\perp$ also $\sigma_\parallel$ is allowed independent adjustment. This is particularly appealing because no sacrifice of an elementary experimental molecular observable is needed. In this case, an automated scheme for parameter optimization, such as, e.g., the method proposed by Stoll,[29] would be most beneficial.

It is apparent from the liquid structure predicted by the model that the quadrupolar interaction is too strong relative to the dispersion interaction. However, decreasing the quadrupolar interaction strength is not feasible for two reasons. First, it would no longer correspond to the theoretical quadrupole moment, and multipoles are, if anything, greater in the liquid phase than in the gas phase because of electronic induction effects. Second, this would further exaggerate the underestimation of the liquid binding energy. Therefore, it seems clear that it must be the dispersion interaction which is to be strengthened, but to keep the good agreement with the vapor−liquid equilibrium, an increase of ε must be counterbalanced by a smaller entropy of the liquid. The most obvious way to bring that about is to increase the steric elongation of the 1CALJQ model.

APPENDIX A. SIMULATION DETAILS

The vapor−liquid coexistence calculations were performed in the Gibbs ensemble algorithm[19] using 712 molecules in total. The total energy is given as the sum over all molecular pairs within a cutoff distance, plus a mean-field contribution, u_{lr}, from the interactions beyond the cutoff range. For the electrostatic interaction, this latter contribution vanishes because of the assumption of random order in the fluid, but for the Lennard-Jones-like interactions the tail energy

$$u_{lr} = \frac{1}{2}\varepsilon\rho\int_{r_c}^{\infty} \mathrm{d}r 4\pi r^2 \left[\left(\frac{\sigma_\perp\langle\phi\rangle}{r}\right)^{12} - \left(\frac{\sigma_\perp\langle\phi\rangle}{r}\right)^{6}\right] \qquad (11)$$

was added for each molecule, where r_c is half the current box length, ρ the number density, and $\langle\phi\rangle = 1 + (1/2)((\sigma_\parallel/\sigma_\perp) - 1)$.

At each temperature between 220 and 290 K, random starting configurations near the experimental coexistence densities were canonically equilibrated for 10^6 cycles. An equilibration using the full Gibbs ensemble algorithm[19] was then carried out for 6.3×10^6 Markov cycles followed by an equal number of cycles for statistical sampling. For the simulation at 295 K, the last configuration of the 290 K simulation was used as a starting point, and 6.3×10^6 steps were taken as equilibration before sampling 6.3×10^6 cycles as per above.

Volume exchanges, particle exchanges, and particle displacements (including rotations) were attempted with 10%, 50%, and 40% probability, respectively, at each Markov step. The acceptance ratio for particle displacements was 40−50%, for particle exchange around 1−4% and for volume exchanges 60−70%. Running on a single Intel Xeon 1.6 GHz core, 50 000 such cycles took about five minutes of real time when compiled with the Intel Fortran 12.0.2 compiler using the "-ip -fast" compiler flags.

For the pair distribution functions, simulations were performed in the canonical ensemble using 512 molecules. Interaction cutoffs were introduced at half the box length. Statistical sampling was carried out over 6×10^6 Monte Carlo cycles, and the data were discretized into "bins", each of 0.1 Å width. For better-looking graphical display, cubic splines were interpolated between these data points before being plotted. The same numerical protocol (512 molecules, canonical simulation) was followed for the supercritical isochore calculations but with equilibration and averaging over 6.3 million cycles at each data point, starting from random fluid arrangements.

All of the Fortran 90 source code for the simulations reported is available upon request.

AUTHOR INFORMATION

Corresponding Author
*E-mail: rasmus.persson@chem.gu.se.

ACKNOWLEDGMENT

Some of the Gibbs ensemble simulations were run on the computer clusters of the Chalmers Centre for Computational Science and Engineering (C^3SE).

REFERENCES

(1) Kihara, T. *Rev. Mod. Phys.* **1953**, *25*, 831.
(2) Koide, A.; Kihara, T. *Chem. Phys.* **1974**, *5*, 34.
(3) Lennard-Jones, J. E. *Proc. R. Soc. London A* **1924**, *106*, 463.
(4) Berne, B. J.; Pechukas, P. *J. Chem. Phys.* **1972**, *56*, 4213.
(5) Toxvaerd, S. *J. Chem. Phys.* **1990**, *93*, 4290.
(6) Lustig, R.; Steele, W. A. *Mol. Phys.* **1988**, *65*, 475.
(7) Ungerer, P.; Beauvais, C.; Delhommelle, J.; Boutin, A.; Rousseau, B.; Fuchs, A. H. *J. Chem. Phys.* **2000**, *112*, 5499.
(8) MacRury, T. B.; Steele, W. A.; Berne, B. J. *J. Chem. Phys.* **1976**, *64*, 1288.

(9) Murthy, C. S.; Singer, K.; McDonald, I. R. *Mol. Phys.* **1981**, *44*, 135.
(10) Murthy, C. S.; Oshea, S. F.; McDonald, I. R. *Mol. Phys.* **1983**, *50*, 531.
(11) Harris, J. G.; Yung, K. H. *J. Phys. Chem.* **1995**, *99*, 12021.
(12) Potoff, J. J.; Panagiotopoulos, A. Z. *J. Chem. Phys.* **1998**, *109*, 10914.
(13) Merker, T.; Engin, C.; Vrabec, J.; Hasse, H. *J. Chem. Phys.* **2010**, *132*, 234512.
(14) Mognetti, B. M.; Yelash, L.; Virnau, P.; Paul, W.; Binder, K.; Müller, M.; MacDowell, L. G. *J. Chem. Phys.* **2008**, *128*, 104501.
(15) Eisenschitz, R.; London, F. *Z. Phys.* **1930**, *60*, 491.
(16) Atkins, P.; Friedman, R. *Molecular Quantum Mechanics*, 4th ed.; Oxford University Press: Oxford, 2005.
(17) Maroulis, G. *Chem. Phys. Lett.* **2004**, *396*, 66.
(18) Haskopoulos, A.; Maroulis, G. *Chem. Phys. Lett.* **2006**, *417*, 235.
(19) Panagiotopoulos, A. Z. *Mol. Phys.* **1987**, *61*, 813.
(20) Span, R.; Wagner, W. *J. Phys. Chem. Ref. Data* **1996**, *25*, 1509.
(21) Lemmon, E. W.; McLinden, M. O.; Friend, D. G. In *NIST Chemistry WebBook, NIST Standard Reference Database Number 69*; Linstrom, P. J., Mallard, W. G., Eds.; National Institute of Standards and Technology: Gaithersburg MD, 20899, 2008; Chapter Thermophysical Properties of Fluid Systems, http://webbook.nist.gov (accessed August 5, 2010)
(22) Harmony, M. D.; Laurie, V. W.; Kuczkowski, R. L.; Schwendeman, R. H.; Ramsay, D. A. *J. Phys. Chem. Ref. Data* **1979**, *8*, 619.
(23) Granar, G.; Rossetti, C.; Bailly, D. *Mol. Phys.* **1986**, *58*, 627.
(24) Cipriani, P.; Nardone, M.; Ricci, F. P. *Phys. B* **1998**, *241−243*, 940.
(25) Bukowski, R.; Sadlej, J.; Jeziorski, B.; Jankowski, P.; Szalewicz, K.; Kucharski, S. A.; Williams, H. L.; Rice, B. M. *J. Chem. Phys.* **1999**, *110*, 3785.
(26) Persson, R. A. X. *J. Chem. Phys.* **2011**, *134*, 034312.
(27) Singh, J. K.; Kofke, D. A. *Phys. Rev. Lett.* **2004**, *92*, 220601.
(28) Dushek, W.; Kleinrahm, R.; Wagner, W. *J. Chem. Thermodyn.* **1990**, *22*, 827.
(29) Stoll, J. *Molecular Models for the Prediction of Thermophysical Properties of Pure Fluids and Mixtures*; VDI-Verlag: Düsseldorf, 2005.